Large Polyoxotitanate Clusters: Well-Defined Models for Pure-Phase TiO2 Structures and Surfaces

5 AUTHORS, INCLUDING:

Jason B Benedict
University at Buffalo, The State University …
69 PUBLICATIONS   **1,129** CITATIONS

Elzbieta Trzop
Université de Rennes 1
33 PUBLICATIONS   **461** CITATIONS

Philip Coppens
University at Buffalo, The State University …
469 PUBLICATIONS   **15,679** CITATIONS

Large Polyoxotitanate Clusters: Well-Defined Models for Pure-Phase TiO₂ Structures and Surfaces

Jason B. Benedict,* Renata Freindorf, Elzbieta Trzop, Jeffrey Cogswell, and Philip Coppens

Department of Chemistry, University at Buffalo, State University of New York, Buffalo, New York 14216

Received July 30, 2010; E-mail: jbb6@buffalo.edu

Abstract: Careful control of the temperature and duration of the reaction between titanium *tert*-butoxide and acetic acid leads to the formation of new polyoxotitanate clusters with 14, 18, and 28 Ti atoms. They are considered intermediates in the growth of Ti/O nanoclusters of increasing size. The Ti₂₈ cluster is the largest crystallized to date. UV/vis spectroscopy on this cluster reveals that the optical band gap is blue-shifted with respect to a cluster containing only 17 titanium atoms indicating that the optical properties are more heavily influenced by the internal structure of the particle than its size.

Precise structural information on surface layers of titanium oxide nanoparticles is generally lacking but can be obtained from crystalline phases of polyoxotitanate (POT) nanoclusters. However, their use has been limited by the size of the clusters which have been synthesized so far. We now report on the synthesis and crystallization of three new phases, which give insight into the structure of the surface layers of Ti/O phases and into the growth mechanism of Ti nanoparticles.

Because of their importance in the design of efficient photovoltaic cells, the properties of photosensitizer dyes adsorbed on Ti/O surfaces have been extensively investigated by both experimental and theoretical methods.[1−5] The crystalline nanocluster phase offers the opportunity to relate spectroscopic and other information on the clusters to the geometry at atomic resolution[6,7] and provides a unique bridge between monomeric metal species and bulk metal oxides in terms of both atomic structure and chemical reactivity. Though molybdenum, tungsten, and vanadium clusters dominate the polyoxometalate (POM) literature,[8] polyoxotitanates have received considerable interest, particularly for their catalytic properties.[9−11] We recently described POTs functionalized with catechol and isonicotinic acid as models for the interface in dye-sensitized solar cells.[7]

Prior to this report, 18 titanium atom clusters were the largest POTs synthesized.[11,12] Here we report the synthesis, crystallization, and structure determination of three new POT clusters: Ti₁₄O₂₀H(OBuᵗ)₁₃(OAc)₄ (**1**), Ti₁₈O₂₅OBuᵗ₁₂OAc₁₀ (**2**), and Ti₂₈O₄₀OBuᵗ₂₀OAc₁₂ (**3**). The Ti₂₈ cluster is the largest POT synthesized and crystallized to date. Bonding in the metal oxide cores of these POT clusters shares features of the bulk pure-phase structures. At the periphery, however, they exhibit undercoordination as expected in the surface layers of the larger Ti/O nanoparticles, the structure of which controls the mode of binding of the dye molecules.

In **1**, 9 of the 14 titanium atoms are six-coordinate with distorted octahedral geometries whereas 4 are five-coordinate possessing a square pyramidal geometry. The remaining titanium atom is four-coordinate with a tetrahedral geometry.

The structure of **2** differs significantly from the two Ti₁₈ structures published previously[11,12] but is remarkably similar to that of **1**. It can be considered as **1** with an additional group of four titanium atoms. Of the 18 titanium atoms in **2**, 15 are six-coordinate and 3 are five-coordinate possessing distorted octahedral and square pyramidal geometries, respectively.

The structure of **3**, also similar to that of **1**, appears to be a pair of 14 titanium atom clusters joined through two Ti-oxygen bridges. Of the titanium atoms in this cluster, 20 are six-coordinate, while the remaining 8 are five-coordinate. The metal oxide core of **3** is 2.0 nm wide, while longest dimension of the entire particle is nearly 2.4 nm.

The structural similarities of the three compounds are illustrated in Figure 1. The three five-coordinate titanium atoms in **2** are located in identical positions in clusters **1** and **3**. The similar positions and orientations of the ligands are clear in the wire frame view. The two acetate groups at the top of the clusters provide a convenient reference for aligning the three clusters relative to one another.
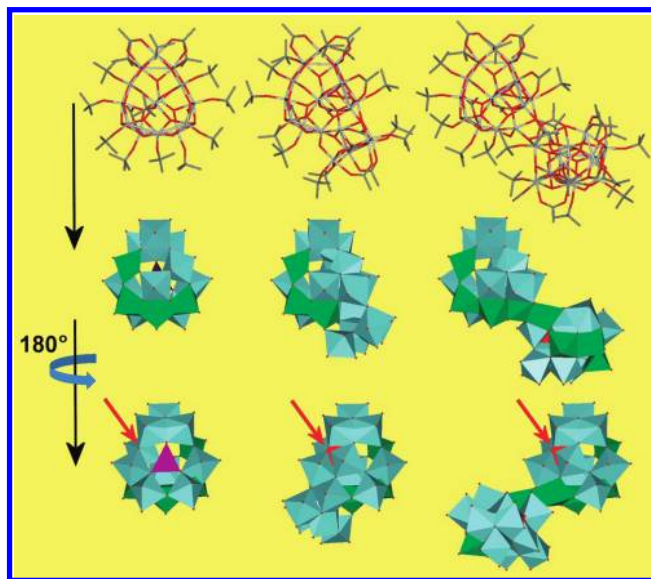

Figure 1. Upper: Wire frame visualization of **1**, **2**, and **3** (left to right). Middle row: Polyhedral representation of the titanium atoms in the metal oxide core shaded according to coordination number: Six (blue), five (green), four (purple). Lower: Same as middle except molecules have undergone a C_2 rotation as indicated. Red arrows indicate the oxygen which is three-coordinate in **1** and four-coordinate in **2** and **3**.

Viewed as polyhedra, it is evident that the majority of the titanium atoms of the common Ti₁₄ fragment share not only the spatial position within the cluster but also the orientation and connectivity of the coordination sphere. In **2** and **3**, the four-coordinate titanium in **1** is displaced sideways and becomes six-coordinate. The acetate group bound to the analogous titanium in

2 and **3** not only contributes a metal oxygen bond but also results in a new bond of the titanium atom with a neighboring oxygen atom increasing the coordination of the oxygen atom to four.

Viewed together, the structures of **1**, **2**, and **3** appear to be snapshots of intermediate structures in the growth of TiO_2 nanoparticles. In fact when the solutions that produce **1**, **2**, and **3** are heated to 160 °C, a white powder insoluble in organic solvents is precipitated (Supporting Information). XRD analysis of the powder revealed it to be anatase (Figure 2). Unlike the commercially available P25 it does not contain a rutile contaminant. It is tempting to presume that the order of cluster formation tracks with the cluster size; i.e., the formation of **1** precedes **2** which is in turn followed by **3**. However, the presence of **2** and **3** in a solution heated for 2 days and **1** and **3** in a solution heated for 5 days suggests the mechanisms of formation to be more complicated. That the larger cluster **2** might form prior to **1** is supported by examining the acetate ratio, the number of acetate ligands to butoxide ligands, in the POT clusters. Of the three complexes presented herein, **2** possesses the largest acetate ratio of 0.83. **3** and **1** have acetate ratios of 0.6 and 0.3, respectively.
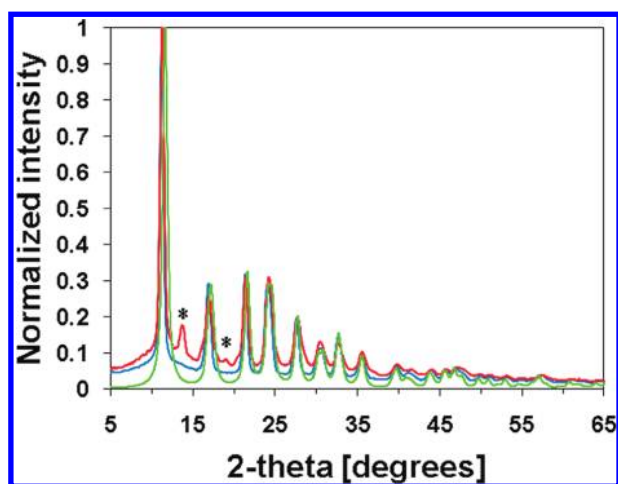

Figure 2. Experimental XRD powder patterns of commercially available TiO_2 (Degussa P25, red line) and powder obtained from reactions at 160 °C (blue line) overlaid with calculated powder pattern for anatase (green line) using Mercury (fwhm = 0.7°). Peaks from rutile present in the commercial powder are indicated by stars.

POT growth is driven by the hydrolysis of the titanium alkoxides by water released from esterification reactions between acetic acid and the butanol. The presence of *tert*-butyl acetate as a solvent of crystallization in the structure of **1** provides direct evidence to support this mechanism. As the reaction proceeds, acetic acid is consumed, and the titanium precursor is hydrolyzed into larger clusters. We hypothesize that a cluster rich in acetate such as **2** is formed earlier in the reaction when the concentration of acetic acid was higher than later when the acetic acid was near depletion.

The crystal structures of rutile,[13] anatase,[14] and brookite,[15] the three common pure-phase polymorphs of TiO_2, consist entirely of six-coordinate titanium atoms connected by μ_3-oxo bridges. That all three clusters presented herein also consist primarily of six-coordinate titanium atoms connected through μ_3-oxo bridges speaks to the structural similarities between these complexes and their pure-phase counterparts. Additionally, fragments of the Ti/O cores strongly resemble the extended structures of rutile and anatase (Supporting Information). However, the clusters also share structural motifs more likely found on TiO_2 surfaces such as undercoordination of titanium, the presence of which has been attributed to the increased reactivity of nanoclusters.[16]

Because of the correlation between the degree of condensation, defined by y/x for $[Ti_xO_y][OR]_{4x-2y}$, and the susceptibility to hydrolysis,[17] the former provides a metric for assessing the stability of a cluster and the similarity to the fully condensed TiO_2. While the degree of condensation generally increases with cluster size, this is not always the case. With a condensation factor (CF) of 1.56, the previously described $[Ti_{18}O_{28}H(OBu^t)_{17}]$[11] remains the most condensed POT to date. Despite **1** possessing twice as many titanium atoms as **3**, both clusters possess equivalent degrees of condensation at 1.43, while **2** which also contains more Ti atoms than **1** is slightly lower with a CF of 1.39. Although we have not tested our compounds' susceptibility to further hydrolysis, based on their similar CFs they likely exhibit a reactivity similar to that of $[Ti_{18}O_{28}H(OBu^t)_{17}]$. It is worth noting that even though progress has been made in growing larger POT clusters, no clusters have yet been identified with a CF between 1.56 and 2.0.
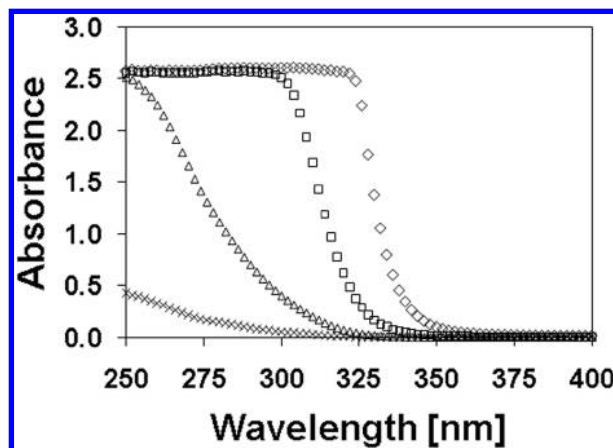

Figure 3. Absorption spectra of **3** in CH_2Cl_2 at the following concentrations: 6.3 (◇), 0.63 (□), 0.063 (△), and 6.3×10^{-3} (×) g/L.

Only **3** could be isolated in quantities sufficient for UV/vis spectroscopy. The spectra of this compound, shown in Figure 3, are remarkably similar to the spectra of the Ti_{17} clusters reported previously.[7] At high loading densities (6.3 g/L), the absorption onset occurs at approximately 350 nm; the onset occurs below 300 nm at loading densities below 6.3×10^{-3} g/L. For optical transitions near the absorption edge the absorption coefficient, α (cm^{-1}), is given by the following expression:

$$\alpha = B(h\nu - E_g)^n/h\nu \qquad (1)$$

where B is the absorption constant for the transition, E_g (eV) the energy of the band gap, and $h\nu$ (eV) the photon energy.[18] The power n characterizes the nature of the transition.

The fit of eq 1 to the absorption coefficient near the absorption edge (Supporting Information) reveals that **3** possesses an allowed direct transition band gap of 4.53 ± 0.02 eV ($R^2 = 0.999$) and a forbidden indirect transition band gap of 3.43 ± 0.01 eV ($R^2 = 0.946$). These values are blue-shifted with respect to both large single crystals and distributions of nanoparticles of pure-phase TiO_2[19] and of monodisperse Ti_{17} clusters.[7] The blue shifts of **3** relative to the direct and indirect band gaps of Ti_{17} which are 4.26 and 3.36 eV, respectively, are noteworthy given the additional 11 titanium atoms and larger cluster size of **3**. One must conclude that the blue shift of **3** is likely the result of the different bonding within the metal oxide core. In accordance with the core of **3** resembling two Ti_{14} fragments connected by only two metal oxygen bonds, it appears to possess electronic properties consistent with those of a smaller cluster.

In conclusion, we present the synthesis and characterization of three new polyoxotitanate nanoclusters. The 28 titanium atom cluster described herein is the largest POT synthesized and crystallized to date. While high temperatures and pressures are required to obtain these clusters, excessive heating results in the exclusive formation of anatase. The well-defined POT clusters possess features of both the pure-phase bulk crystal structures and their surfaces, making POTs unique analogs for pure-phase nanoparticles. The larger energy band gap of the Ti_{28} cluster relative to the Ti_{17} cluster indicates that the optical properties are determined not by the size of the particle but rather the nature of the bonding within the semiconductor core.

Supporting Information Available: Additional discussion of structures; preparation details of **1**, **2**, and **3**; experimental details; additional figures; crystallographic data of **1**, **2**, and **3**; and CIF file. This material is available free of charge via the Internet at http://pubs.acs.org.

References

(1) Duncan, W. R.; Prezhdo, O. V. *Annu. Rev. Phys. Chem.* **2007**, *58*, 143–84.

(2) Persson, P.; Lunell, S.; Bruhwiler, P. A.; Schnadt, J.; Sodergren, S.; O'Shea, J. N.; Karis, O.; Siegbahn, H.; Martensson, N.; Bassler, M.; Patthey, L. *J. Chem. Phys.* **2000**, *112*, 3945–3948.

(3) Persson, P.; Lundqvist, M. J. *J. Phys. Chem. B* **2005**, *109*, 11918–11924.

(4) Lundqvist, M. J.; Nilsing, M.; Lunell, S.; Akermark, B.; Persson, P. *J. Phys. Chem. B* **2006**, *110*, 20513–20525.

(5) Lundqvist, M. J.; Nilsing, M.; Persson, P.; Lunell, S. *Int. J. Quantum Chem.* **2006**, *106*, 3214–3234.

(6) Soloviev, V. N.; Eichhofer, A.; Fenske, D.; Banin, U. *J. Am. Chem. Soc.* **2001**, *123*, 2354–2364.

(7) Benedict, J. B.; Coppens, P. *J. Am. Chem. Soc.* **2010**, *132*, 2938–2944.

(8) Long, D.-L.; Burkholder, E.; Cronin, L. *Chem. Soc. Rev.* **2007**, *36*, 105–121.

(9) Day, V. W.; Eberspacher, T. A.; Klemperer, W. G.; Park, C. W. *J. Am. Chem. Soc.* **1993**, *115*, 8469–8410.

(10) Steunou, N.; Kickelbick, G.; Boubekeur, K.; Sanchez, C. *J. Chem. Soc., Dalton Trans.* **1999**, 3653–3655.

(11) Campana, C. F.; Chen, Y.; Day, V. W.; Klemperer, W. G.; Sparks, R. A. *J. Chem. Soc., Dalton Trans.* **1996**, 691–702.

(12) Toledano, P.; In, M.; Sanchez, C. *C. R. Acad. Sci. Paris* **1991**, *313*, 1247–1253.

(13) Baur, W. H.; Khan, A. A. *Acta Crystallogr.* **1971**, *B27*, 2133–2139.

(14) Horn, M.; Schwertfeger, C. F.; Meagher, E. P. *Z. Kristallogr.* **1972**, *136*, 273–281.

(15) Baur, W. H. *Acta Crystallogr.* **1961**, *A14*, 214–216.

(16) Li, G.; Dimitrijevic, N. M.; Chen, L.; Nichols, J. M.; Rajh, T.; Gray, K. A. *J. Am. Chem. Soc.* **2008**, *130*, 5402–5403.

(17) Day, V. W.; Eberspacher, T. A.; Chen, Y.; Hao, J.; Klemperer, W. G. *Inorg. Chim. Acta* **1995**, *229*, 391–405.

(18) Adachi, S. *Optical properties of crystalline and amorphous semiconductors: Materials and fundamental principles*; Springer: 1999.

(19) Serpone, N.; Khairutdinovt, D. L. a. R. *J. Phys. Chem.* **1995**, *99*, 16646–16654.

JA106436Y